RSC Advances

ROYAL SOCIETY OF CHEMISTRY

www.rsc.org/advances

Stereocomplexation of Quaternary or Ternary Monomer Units and Dual Stereocomplexation in Enantiomeric Binary and Quaternary Polymer Blends of Poly(2-hydroxybutanoic acid), Poly(2-hydroxybutanoic acid-*co*-lactic acid)s, and Poly(lactic acid)

Hideto Tsuji[*] *and Tadashi Sobue*

Department of Environmental and Life Sciences, Graduate School of Engineering, Toyohashi University of Technology, Tempaku-cho, Toyohashi, Aichi 441-8580, Japan

E-mail: tsuji@ens.tut.ac.jp

Abstract: The solution- and melt-crystallized binary polymer blends from L- and D-configured poly(2-hydroxybutanoic acid) homopolymers [P(L-2HB) and P(D-2HB), respectively], L- and D-configured poly(2-hydroxybutanoic acid-co-lactic acid) random copolymers [P(L-2HB-LLA) and P(D-2HB-DLA), respectively], and L- and D-configured poly(lactic acid) homopolyemrs (PLLA and PDLA, respectively) and the solution- and melt-crystallized quaternary polymer blend of P(L-2HB), P(D-2HB), PLLA, and PDLA were prepared and their crystallization behavior was investigated by wide-angle X-ray diffractometry (WAXD), differential scanning calorimetry, and polarized optical microscopy. The WAXD profiles and the interplane distance values first revealed the stereocomplexation of quaternary or ternary monomer units of optically active 2-hydroxybutanoic acid and lactic acid units in binary polymer blends of the copolymer with the copolymer or the homopolymer and the dual homo-stereocomplexation of P(L-2HB) and P(D-2HB) and of PLLA and PDLA in the quaternary homopolymer blends.

Keywords: poly(lactide); poly(hydroxybutyrate); stereocomplexation

1 Introduction

Biodegradable polyesters are utilized for biomedical, pharmaceutical, and environmental applications, because of their biodegradability and very low toxicity in the human body and the environment, and high mechanical performance.[1–10] Among the biodegradable polyesters, especially poly(hydroxyalkanoic acid)-based biodegradable polyesters such as poly(lactide)s [i.e., poly(lactic acid)s, PLAs, -(-O-CH(CH_3)-CO-)$_n$-] are intensively investigated. Binary homo-stereocomplex (HMSC) formation is reported for enantiomeric L- and D-configured biodegradable polyesters, such as poly(2-hydroxymethyl-2-methylbutanoic acid) or poly(α-methyl-α-ethyl-β-propiolactone)s,[11] poly(3-hydroxy-4,4-dichloropentanoic acid) and poly(3-hydroxy-4,4-dichlorohexanoic acid) with different side groups containing chlorides,[12] PLAs [13–20], poly(2-hydroxybutyrate) [i.e., poly(2-hydroxybutanoic acid)s, P(2HB)s, -(-O-CH(CH_2CH_3)-CO-)$_n$-],[21–23] and poly(2-hydroxy-3-methylbutyrate) [i.e., poly(2-hydroxy-3-methylbutanoic acid)s, P(2H3MB)s, -(-O-CH(CH(CH_3)$_2$)-CO-)$_n$-].[24]

Binary homo-stereocomplexation enhances mechanical performance, hydrolytic/thermal degradation resistance, gas barrier properties compared to those of neat polymers.[15,22,25–28] Of homo-stereocomplexation of enantimoeric polyesters, that of PLLA/PDLA blends[29–48] and stereoblock PLAs[49–70] highly attracts the interest of macromolecular researchers. On the other hand, binary hetero-stereocomplex (HTSC) is formed between P(2HB) and PLA[71–74] or P(2H3MB)[75] with different types of side chains and opposite configurations.

Ternary stereocomplex (TSC) formation is reported for L- and D-configured P(2HB)s and L- or D-configured PLA[76,77] and also quaternary stereocomplex (QSC) formation is reported for L- and D-configured P(2HB)s and L- and D-configured P(2H3B)s.[78] However, these reported stereocomplexes (SCs) are based on enantiomeric homopolymers and stereoblock copolymers but not on the enantiomeric random copolymers. Recently, we first found that the interesting and unique cocrystallization of monomer units can occur in L-configure random copolymers composed of L-2-hydroxybutanoic acid and L-lactic acid and [P(L-2HB-*co*-LLA)] for a wider L-2-hydroxybutanoic

acid unit content range of 27–74 mol%.[79] The cocrystallization even in the comonomer unit range around 50 mol% strongly suggests that the cocrystallization occurs at an arbitrary comonomer unit content. From this result, it is expected that the monomer units in random copolymers composed of both optically active D-lactic acid and D-2-hydroxybutanoic acid [P(DLA-*co*-D-2HB)] are also cocrystallizable and that SC containing quaternary monomer units in the stereocomplex crystalline regions can be formed by blending L-configured P(LLA-*co*-L-2HB) copolymer with D-configured P(DLA-*co*-D-2HB) copolymer and that SC containing ternary monomer units in the stereocomplex crystalline regions can be formed by blending D-configured P(DLA-*co*-D-2HB) copolymer with L-configured poly(L-2-hydroxybutanoic acid) [P(L-2HB)] homopolymer or poly(L-lactic acid) (PLLA) homopolymer and by blending L-configured P(LLA-*co*-L-2HB) copolymer with D-configured poly(D-2-hydroxybutanoic acid) [P(D-2HB)] homopolymer or poly(D-lactic acid) (PDLA) homopolymer. Also, to the best of our knowledge, QSC formation in the quaternary homopolymer blends of P(L-2HB), P(D-2HB), PLLA, and PDLA has not been reported so far.

The purpose of the present study was to investigate such stereocomplexationability of quaternary or ternary monomer units in enantiomeric binary polymer blends of the copolymer with the copolymer or the homopolymer and of stereocomplexationability in the enantiomeric quaternary homopolymer blend. For this purpose, we synthesized optically active random copolymers, P(LLA-*co*-L-2HB) and P(DLA-*co*-D-2HB), together with optically active homopolymers, P(L-2HB), P(D-2HB), PLLA, and PDLA, prepared various types of solution- and melt-crystallized enantiomeric binary polymer blends of copolymer/copolymer (C), copolymer/homopolymer (B and D), and homopolymer/homopolymer (A and E), and enantiomeric quaternary polymer blend of homopolyemers, P(L-2HB), P(D-2HB), PLLA, and PDLA (F) (Figure 1), and investigated the crystallization behavior in the enantiomeric binary and quaternary polymer blends using wide-angle X-ray diffractometry (WAXD), differential scanning calorimetry (DSC), and polarized optical microscopy (POM).

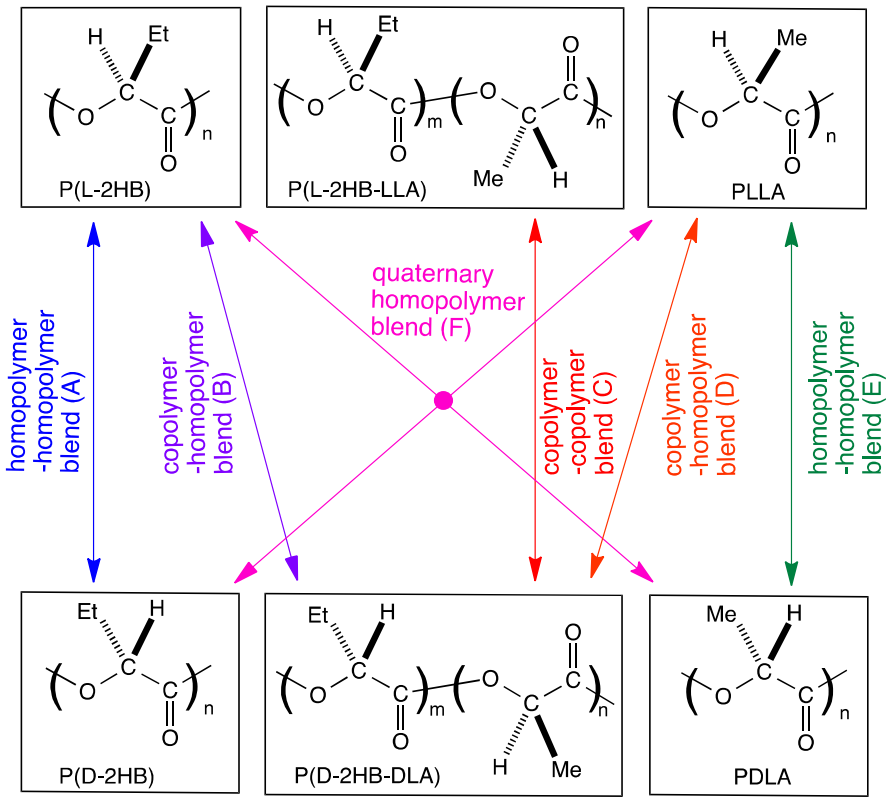

Figure 1. Molecular structures of poly(L-2-hydroxybutanoic acid) [P(L-2HB)], poly(D-2-hydroxybutanoic acid) [P(D-2HB)], poly(L-2-hydroxybutanoic acid-L-lactic acid) [P(L-2HB-LLA)], and poly(D-2-hydroxybutanoic acid- D-lactic acid) [P(D-2HB-DLA)], poly(L-lactic acid) (PLLA), and poly(D-lactic acid) (PDLA), and their combinations for blends. (A), (B), (C), (D), and (E) correspond to the blend codes in the present study.

2 Experimental Section

2.1 Materials

P(L-2HB), P(D-2HB), P(LLA-*co*-L-2HB), P(DLA-*co*-D-2HB), PLLA, and PDLA were synthesized by polycondensation of L-2-hydroxybutanoic acid [(*S*)-2-hydroxybutyric acid] (≥ 97.0%, Sigma-Aldrich Co., Tokyo, Japan), and D-2-hydroxybutanoic acid [(*R*)-2-hydroxybutyric acid] (≥ 98.0%, Sigma-Aldrich Co.), L-lactic acid prepared by hydrolytic degradation of L-lactide (PURASORB L®, Purac B iomaterials, Gorinchem, The Netherlands), and D-lactic acid prepared by hydrolytic degradation of D-lactide (PURASORB D®, Purac Biomaterials), using 5wt%

p-toluenesulfonic acid (monohydrate, guaranteed grade, Nacalai Tesque inc., Kyoto, Japan) as the catalyst, as reported previously.[80,81] The reaction was performed at 130°C under atmospheric pressure for 5 h for the synthesis of all polymers and then under reduced pressure of 1.4 kPa for 9 h for the synthesis of P(L-2HB) and P(D-2HB), of 1.8–1.9 kPa for 24 h for the synthesis of P(LLA-*co*-L-2HB) and P(DLA-*co*-D-2HB), and of 0.9–2.0 kPa for 24 h for the synthesis of PLLA and PDLA. The L- and D-lactic acids used for polymer synthesis were prepared by hydrolytic degradation of L- and D-lactides, respectively, with distillated water [L- or D-lactide/water (mol/mol) = 1/12] at 98°C for 30 min. The synthesized polymers were purified by reprecipitation using chloroform and methanol (both guaranteed grade, Nacali Tesque Inc.) as the solvent and nonsolvent, respectively. The purified polymers were dried under reduced pressure for at least 6 days. The molecular characteristics of the polymer used in the present study are summarized in Table 1.

Table 1. Molecular characteristics of polymers used in the present study.

Polymer	M_w [a] (g mol^{-1})	M_w/M_n [a]	$[\alpha]^{25}_{589}$ [b] (deg dm^{-1} g^{-1} cm^3)	*2HB unit content* (mol%)[c]
P(L-2HB)	1.32×10^4	1.37	-111	-
P(D-2HB)	1.31×10^4	1.42	111	-
P(L-2HB-LLA)	1.39×10^4	1.30	-131	44.0
P(D-2HB-DLA)	1.63×10^4	1.50	129	48.2
PLLA	1.44×10^4	1.68	-157	-
PDLA	1.88×10^4	1.72	150	-

[a] M_w and M_n are weight- and number-average molecular weights, respectively, estimated by GPC.
[b] Measured in chloroform.
[c] 2-Hydroxybutanoic acid (2HB) unit content estimated by ^{1}H NMR according to the method reported in refs. 72 and 79.

Table 2. Binary and quaternary polymer blends prepared in the present study.

Blend	Blend code	Polymer composition (mol%)						*Type number of polymer*	*Type number of monomer unit*	*2HB unit content* [a] (mol%)
		P(L-2HB)	PLLA	P(L-2HB-LLA)	P(D-2HB)	PDLA	P(D-2HB-DLA)			
P(L-2HB)/P(D-2HB)	A	50	0	0	50	0	0	2	2	100.0
P(L-2HB)/P(D-2HB-DLA)	B	50	0	0	0	0	50	2	3	74.1
P(L-2HB-LLA)/P(D-2HB-DLA)	C	0	0	50	0	0	50	2	4	46.1
PLLA/P(D-2HB-DLA)	D	0	50	0	0	0	50	2	3	24.1
PLLA/PDLA	E	0	50	0	0	50	0	2	2	0.0
P(L-2HB)/P(D-2HB)/PLLA/PDLA	F	25	25	0	25	25	0	4	4	50.0

[a] 2-Hydroxybutanoic acid (2HB) unit content.

Equimolar binary polymer blend were prepared by the procedure stated in the previous pape.[21,71,75] Briefly, each solution of the two enantiomeric polymers was prepared separately to have a polymer concentration of 1.0 g dL^{-1} and then admixed with each other equimolarly under vigorous stirring. Dichloromethane (guaranteed grade, Nacali Tesque Inc.) was used as the solvent. The mixed solution was cast onto a petri-dish, followed by solvent evaporation at 25°C for approximately one day. The obtained polymer blends were further dried under reduced pressure at least 6 days. The quaternary polymer blend of P(L-2HB), and P(D-2HB), PLLA, and PDLA with content of P(L-2HB)/P(D-2HB)/PLLA/PDLA=25/25/25/25(mol/mol/mol/mol) was prepared by mixing separately prepared solutions of the equimolar P(L-2HB)/P(D-2HB) blend and PLLA/PDLA blend using mixed solvent of dichloromethane and 1,1,1,3,3,3-hexafluoro-2-propanol [95/5 (v/v)] and chloroform, respectively, and casting onto a petri-dish, followed by solvent evaporation at 25°C for approximately one day.[78] The obtained quaternary polymer blends were further dried under reduced pressure at least 6 days. We call the thus-prepared blends "solution-crystallized blends". The details of the binary and quaternary polymer blends prepared in the present studies are tabulated in Table 2.

The melt-crystallization of the solution-crystallized blends sealed in test tubes under reduced pressure was performed at a crystallization temperature (T_c) of 160°C for 1 h after melting at 240°C for 2 min. The blends after crystallization were quenched at 0°C to stop further crystallization for at least 5 min. The T_c of 160°C was selected because this T_c has been successfully utilized for

heterostereocomplexation of PLLA/P(D-2HB) or PDLA/P(L-2HB)[71,73] and quaternary stereocomplexation of P(L-2HB)/P(D-2HB)/P(L-2H3MB)/P(D-2H3MB)[78] to avoid homo-crystallization of constituent polymers. We call the thus-prepared blends "melt-crystallized blends".

2.2 Physical measurements and observation

The weight- and number-average molecular weights (M_w and M_n, respectively) of the polymers were evaluated in chloroform at 40°C using a Tosoh (Tokyo, Japan) GPC system with two TSK gel columns (GMH_{XL}) and polystyrene standards. Therefore, the M_w and M_n values are given relative to polystyrene. The specific optical rotation ($[\alpha]^{25}_{589}$) of the polymers was measured in chloroform at a concentration of 1 g dL^{-1} and 25°C using a JASCO P-2100 polarimeter at a wave length of 589 nm. The glass transition, cold crystallization, and melting temperatures (T_g, T_{cc}, and T_m, respectively) and the enthalpies of cold crystallization and melting (ΔH_{cc} and ΔH_m, respectively) were determined with a Shimadzu (Kyoto, Japan) DSC-50 differential scanning calorimeter under a nitrogen gas flow at a rate of 50 mL min^{-1}. The samples (ca. 3 mg) were heated from 0 to 250˚C at a rate of 10°C min^{-1}. WAXD was carried out at 25˚C using a RINT-2500 (Rigaku Co., Tokyo, Japan) equipped with a Cu-K_α source [wave length (λ) = 1.5418 Å]. The isothermal spherulite growth of the samples was observed using an Olympus (Tokyo, Japan) polarized optical microscope (BX50) equipped with a heating-cooling stage and a temperature controller (LK-600PM, Linkam Scientific Instruments, Surrey, UK) under a constant nitrogen gas flow. The samples were heated from room temperature to 240°C at 100°C min^{-1}, held at this temperature for 2 min, cooled at 100°C min^{-1} to T_c of 160°C, and then held at the same temperature (spherulite growth was observed here).

3 Results and Discussion

3.1 Wide-angle X-ray diffractometry

For the estimation of crystalline species and crystallinity of the blends, WAXD measurements were performed. Figure 2 shows the WAXD profiles of the binary blends of copolymers and homopolymers (A–E) and quaternary blend of homopolymers (F). For solution- and melt-crystallized P(L-2HB)/P(D-2HB) binary polymer blend (A), only P(L-2HB)/P(D-2HB) HMSC crystalline diffraction peaks were observed at 2θ values of around 10.8, 18.6, 19.4, and 21.6°,[21–23] whereas for the solution- and melt-crystallized PLLA/PDLA binary polymer blend (E), only PLLA/PDLA HMSC crystalline diffraction peaks were observed at 2θ values of around 11.9, 20.8, and 24.0°.[13,15] These results indicate that solely HMSC crystallites were formed without formation of homo-crystallites of the constituent monomer units of the polymers, which main crystalline diffractions were observed at 17 and 19° for neat PLLA or PDLA and 15 and 17° for neat P(L-2HB) or P(D-2HB).[72,79,82,83] For other binary polymer blends, P(L-2HB)/P(D-2HB-DLA) blend (B), P(L-2HB-LLA)/P(D-2HB-DLA) blend (C), PLL/P(D-2HB-DLA) blend (D), the crystalline diffraction profiles, which shapes are very similar to those of P(L-2HB)/P(D-2HB) and PLLA/PDLA HMSC crystallites, were observed at 2θ values between those of P(L-2HB)/P(D-2HB) and PLLA/PDLA HMSC crystallites, i.e., at 2θ values of 10.8–11.9°, 18.6–20.8°, and 21.6–24.0°. Very interestingly, these findings strongly suggest that stereocomplexation of quaternary monomer units in P(L-2HB-LLA)/P(D-2HB-DLA) blend and of ternary monomer units in P(L-2HB)/P(D-2HB-DLA) and PLLA/P(D-2HB-DLA) blends. On the other hand, the P(L-2HB)/P(D-2HB)/PLLA/PDLA quaternary polymer blend (F) had two series of HMSC diffraction peaks very similar to P(L-2HB)/P(D-2HB) and PLLA/PDLA HMSC crystallites in P(L-2HB)/P(D-2HB) and PLLA/PDLA binary polymer blends, respectively, although for the solution-crystallized sample, the diffraction peaks around 12 and 24° ascribed to PLLA/PDLA HMSC crystallites appeared at lower angles compared to those of PLLA/PDLA binary polymer blend. This result strongly suggests that although the incorporation of P(L-2HB) and P(D-2HB) in PLLA/PDLA HMSC crystallites are suggested for the solution-crystallized sample, dual P(L-2HB)/P(D-2HB) and PLLA/PDLA HMSC crystallites were formed but the complete single QSC formation as reported for P(L-2HB)/P(D-2HB)/P(L-2H3MB)/P(D-2H3MB) quaternary polymer blends, wherein the 2θ values

had linear dependence on the polymer composition, was not formed for P(L-2HB)/P(D-2HB)/PLLA/PDLA quaternary polymer blend.

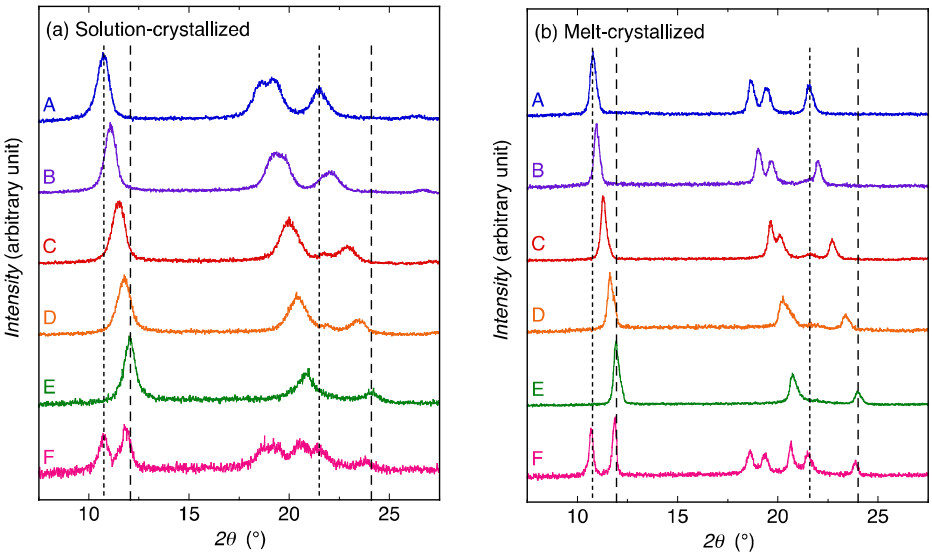

Figure 2. WAXD profiles of solution-crystallized (a) and melt-crystallized (T_c = 160°C) (b) binary polymer blends (A–E) and quaternary polymer blend (F). A: P(L-2HB)/P(D-2HB) blend, B: P(L-2HB)/P(D-2HB-DLA) blend, C: P(L-2HB-LLA)/P(D-2HB-DLA) blend, D: PLLA/P(D-2HB-DLA) blend, E: PLLA/PDLA blend, F: P(L-2HB)/P(D-2HB)/PLLA/PDLA blend. Dotted and broken lines indicate the crystalline diffraction angles for P(L-2HB)/P(D-2HB) and PLLA/PDLA HMSC crystallites, respectively.

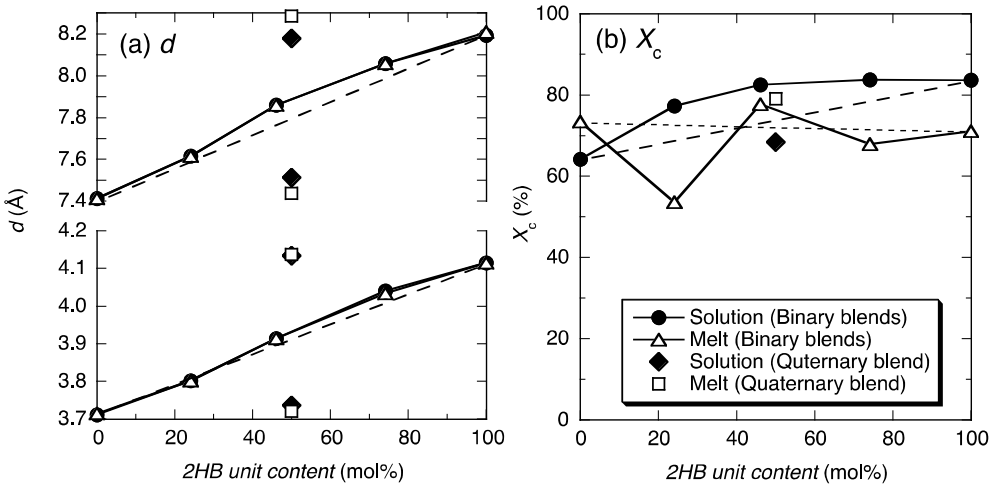

Figure 3. Interplane distance (d) (a) and crystallinity (X_c) (b) of solution- and melt-crystallized (T_c = 160°C) blends in the ranges of 7.4–8.3 and 3.7–4.2Å as a function of 2HB unit content. The theoretical d values are shown in Figure 3(a) with broken lines, whereas the theoretical X_c values are

shown in Figure 3(b) with broken and dotted lines for the solution- and melt-crystallized blends, respectively.

The interplane distance (*d*) values of stereocomplex crystallites of the blends were estimated from the WAXD profiles in Figure 2 and are plotted in Figure 3(a) as a function of 2-hydroxybutanoic acid (2HB) unit content. Due to the shape change from double diffraction peak to single diffraction peak in the 2θ range of 18.6–20.8° with decreasing 2HB unit content, *d* values were estimated for the 2θ ranges of 10.8–11.9° and 21.6–24.0°. The *d* values of solution- and melt-crystallized samples of the binary polymer blends (A–E) increased linearly with 2HB unit content in blends from 3.71 and 7.41Å of PLLA/PDLA HMSC crystallites at 2HB unit content of 0% [PLLA/PDLA blend (E)] to 4.11 and 8.19 (or 8.21) Å of P(L-2HB)P(D-2HB) HMSC crystallites at 2HB unit content of 100% [P(L-2HB)/P(D-2HB) blend (A)], confirming the stereocomplexation of quaternary or ternary monomer units in the PLLA/P(D-2HB-DLA), P(L-2HB-LLA)/P(D-2HB-DLA), and P(L-2HB)/P(D-2HB-DLA) binary polymer blends (B, C, and D). To the best of our knowledge, this is the first report on stereocomplexation between enantiomeric copolymers and between enantiomeric copolymer and homopolymer, wherein all types of quaternary or ternary monomer units cocrystallize. The *d* values of solution- and melt-crystallized samples were very similar with each other, reflecting the very small effects of crystallization procedure on the *d* values. The *d* values of the solution- and melt-crystallized PLLA/P(D-2HB-DLA), P(L-2HB-LLA)/P(D-2HB-DLA), and P(L-2HB)/P(D-2HB-DLA) binary polymer blends at 2HB unit contents of 24.1, 46.1, and 74.1 mol% were higher than theoretical values. The theoretical values were calculated from the experimental *d* values of PLLA/PDLA and P(L-2HB)/P(D-2HB) HMSC crystallites in the solution-crystallize PLLA/PDLA and P(L-2HB)/P(D-2HB) binary polymer blends at 2HB unit contents of 0 and 100 mol%, respectively, assuming the linear dependence of *d* on 2HB unit content. The theoretical values are shown in broken lines in Figure 3(a). This finding reflects the predominant incorporation of 2HB unit rather than lactic acid (LA) unit in these binary polymer blends. On the other hand, quaternary blend (F) at 2HB unit content of 50% had the two *d* values of 3.74 and 4.13 Å and of 7.51 and 8.18 Å for the

solution crystallized sample and of 3.72 and 4.13 Å and of 7.44 and 8.28 Å for the melt-crystallized sample. These two set of values are correspondingly attributed to P(L-2HB)/P(D-2HB) and PLLA/PDLA HMSC crystallites but not to the QSC crystallites. This again confirms the separate and dual formation of P(L-2HB)/P(D-2HB) and PLLA/PDLA HMSC crystallites.

The X_c values of blends were evaluated from the WAXD profiles in Figure 2 and are plotted in Figure 3(b) as a function of 2HB unit content. The X_c values for the solution-crystallized binary blends of PLLA/PDLA and P(L-2HB)/P(D-2HB) at 2HB unit contents of 0 and 100 mol% were 64.2 and 83.7 %, respectively. On the other hand, the X_c values of the solution-crystallized PLLA/P(D-2HB-DLA), P(L-2HB-LLA)/P(D-2HB-DLA), and P(L-2HB)/P(D-2HB-DLA) binary polymer blends at 2HB unit contents of 24.1, 46.1, and 74.1 mol% were higher than theoretical values. The theoretical values were calculated from the experimental X_c values of the solution-crystallized PLLA/PDLA and P(L-2HB)/P(D-2HB) HMSC crystallites in the solution-crystallized PLLA/PDLA and P(L-2HB)/P(D-2HB) binary polymer blends at 2HB unit contents of 0 and 100 mol%, respectively, assuming that two types of HMSC crystallites are formed without interaction with each other. The theoretical values are shown in Figure 3(b) with broken and dotted lines for the solution- and melt-crystallized blends, respectively. The finding here means that the stereocomplexation of quaternary or ternary monomer units readily took place in the solution-crystallized binary polymer blends. The X_c value of the solution-crystallized quaternary homopolymer blend (68.4%) was slightly lower than the theoretical value, indicating the either or both of crystallization of HMSCs were disturbed by the presence of another enantiomeric polymer pair.

The X_c values of the melt-crystallized blends had complicated dependence on 2HB unit content. That is, the X_c values for the melt-crystallized PLLA/PDLA and P(L-2HB)/P(D-2HB) binary polymer blends at 2HB unit contents of 0 and 100 mol% were 73.4 and 71.1 %, respectively. On the other hand, the X_c values of the melt-crystallized PLLA/P(D-2HB-DLA), P(L-2HB-LLA)/P(D-2HB-DLA) and P(L-2HB)/P(D-2HB-DLA) binary polymer blends and at 2HB unit contents of 24.1, 46.1 and 74.1 mol% were respectively lower, slightly higher, and slightly lower than theoretical values. The

theoretical values were calculated from the experimental X_c values of PLLA/PDLA and P(L-2HB)/P(D-2HB) HMSC crystallites in the melt-crystallized PLLA/PDLA and P(L-2HB)/P(D-2HB) binary polymer blends at 2HB unit contents of 0 and 100 mol%. The lower X_c values of the melt-crystallized P(L-2HB)/P(D-2HB-DLA) and PLLA/P(D-2HB-DLA) binary polymer blends at 2HB unit contents of 24.1 and 74.1mol% should be due to low miscibility between PLLA or P(L-2HB) and P(D-2HB-DLA), as can be expected from phase-separation of hetero-stereocomplexationable P(L-2HB)/PDLA or P(D-2HB)/PLLA blend.[71,73] In the case of the solution-crystallized blends such phase-separation should have been avoided by the presence of the solvent. On the other hand, for the solution- and melt-crystallized quaternary polymer blends at 2HB unit contents of 50 mol%, X_c values were 54.2 and 68.8 %, respectively, which are slightly lower and higher than the theoretical values.

The WAXD results here first revealed the stereocomplexation of quaternary or ternary monomer units in enantiomeric binary polymer blends containing the copolymer composed of optically active 2HB and LA units [P(L-2HB)/P(D-2HB-DLA), P(L-2HB-LLA)/P(D-2HB-DLA), and PLL/P(D-2HB-DLA) blends] and the dual stereocomplxation in P(L-2HB)/P(D-2HB)/PLLA/PDLA quaternary homopolymer blend. Also, the X_c values of solution-crystallized binary polymer blends composed of at least one copolymer were higher than or comparable with the theoretical values, whereas the X_c values of melt-crystallized binary polymer blends composed of the homopolymer and the copolymer [P(L-2HB)/P(D-2HB-DLA) and PLL/P(D-2HB-DLA) blends] were lower than the theoretical values and the X_c value of the melt-crystallized binary polymer blend composed of two copolymers [P(L-2HB-LLA)/P(D-2HB-DLA) blend] was comparable with the theoretical value. The X_c values of the solution- and melt-crystallized quaternary homopolymer blends were respectively slightly lower and higher than those of the theoretical values.

3.2 Differential scanning calorimetry

For the estimation of thermal properties of the blends, DSC measurements were carried out (Figure 4).

Only melting peaks of stereocomplex crystallites were observed in the range of 193.4–217.8°C for the most melt- and solution-crystallized blends, except for the melting peaks of P(L-2HB) homo-crystallites in the melt-crystallized P(L-2HB)/P(D-2HB-DLA) blend (B) (101.0°C) (Figure S1) and PLLA homo-crystallites in melt-crystallized PLLA/P(D-2HB-DLA) blend (D) (166.4°C). These melting peaks of homo-crystallites can be ascribed to those formed during DSC heating. This can be evidence by the cold crystallization peaks of P(L-2HB) homo-crystallites (80.2°C) and PLLA (84.9°C) in the melt-crystallized P(L-2HB)/P(D-2HB-DLA) blend (B) and melt-crystallized PLLA/P(D-2HB-DLA) blend (D), respectively (Figure S1) and the very similar peak areas of cold crystallization and melting. Due to the presence of two types of HMSC formation in the quaternary polymer blend (F), the melting peak with large shoulder on the higher temperature side and the double melting peak were observed for the solution- and melt-crystallized samples, respectively. The thermal properties estimated from the DSC thermograms in Figure 5. The thermal properties thus obtained are summarized in Table 3 and the T_m and $\Delta H_c + \Delta H_m$ of the blends are plotted in Figure 5(a) and (b) as a function of 2HB unit content.

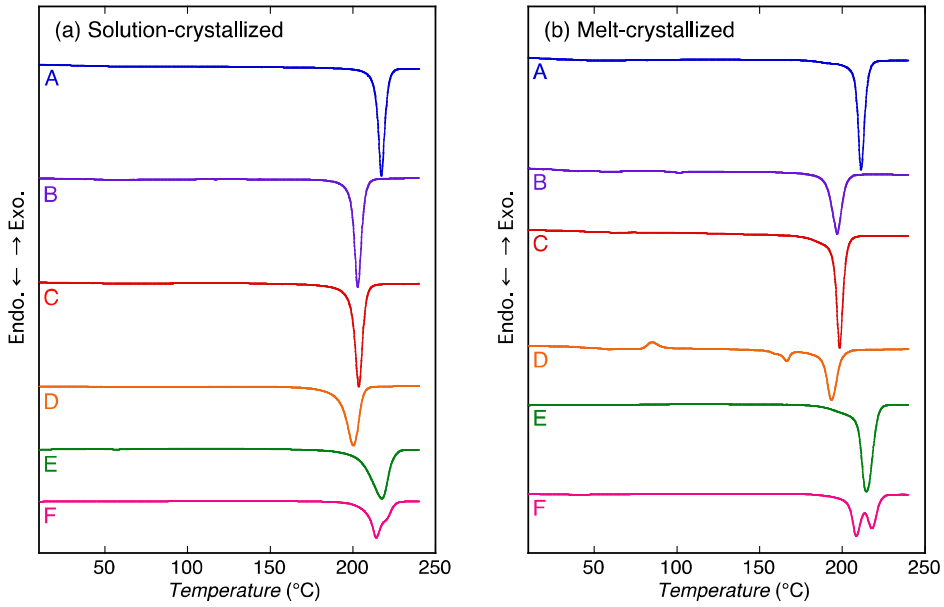

Figure 4. DSC thermograms of solution-crystallized (a) and melt-crystallized (T_c = 160°C) (b) binary polymer blends (A–E) and quaternary polymer blend (F). A: P(L-2HB)/P(D-2HB) blend, B:

P(L-2HB)/P(D-2HB-DLA) blend, C: P(L-2HB-LLA)/P(D-2HB-DLA) blend, D: PLLA/P(D-2HB-DLA) blend, E: PLLA/PDLA blend, F: P(L-2HB)/P(D-2HB)/PLLA/PDLA blend.

Table 3. Thermal properties during heating and crystallinity of neat P(L-2H3MB), P(2-2H3MB), and their blends.

[a] T_g, T_{cc}, and T_m are glass transition, cold crystallization, and melting temperatures, respectively.
[b] ΔH_{cc} and ΔH_m are enthalpies of cold crystallization and melting, respectively.
[c] $\Delta H(\text{tot}) = \Delta H_{cc} + \Delta H_m$.

Crystallization	Blend	Blend code	*2HB unit content* (mol%)	T_g [a] (°C)	T_{cc} [a] (°C)	T_m [a] (°C)	ΔH_{cc} [b] (J g^{-1})	ΔH_m [b] (J g^{-1})	ΔH(tot) [c] (J g^{-1})	X_c [d] (%)
Solution	P(L-2HB)/P(D-2HB)	A	100.0	-	-	217.2	0.0	69.9	69.9	72.3
	P(L-2HB)/P(D-2HB-DLA)	B	74.1	36.5	-	202.8	0.0	78.4	78.4	74.0
	P(L-2HB-LLA)/P(D-2HB-DLA)	C	46.1	42.0	-	203.6	0.0	83.7	83.7	69.0
	PLLA/P(D-2HB-DLA)	D	24.1	37.7, 60.1	-	200.2	0.0	77.1	77.1	66.3
	PLLA/PDLA	E	0.0	48.9	-	217.4	0.0	82.2	82.2	58.2
	P(L-2HB)/P(D-2HB)/PLLA/PDLA	F	50.0	-	-	214.0	0.0	51.5	51.5	54.2
Melt	P(L-2HB)/P(D-2HB)	A	100.0	-	-	211.3	0.0	68.3	68.3	66.7
	P(L-2HB)/P(D-2HB-DLA)	B	74.1	24.6, 35.7	80.2	101.0, 196.7	-0.7	49.7	49.0	62.2
	P(L-2HB-LLA)/P(D-2HB-DLA)	C	46.1	37.0, 58.1	-	198.4	0.0	74.3	74.3	70.2
	PLLA/P(D-2HB-DLA)	D	24.1	37.0, 52.0	84.9	166.4, 193.4	-6.1	57.2	51.1	49.0
	PLLA/PDLA	E	0.0	46.3	-	214.6	0.0	88.2	88.2	68.7
	P(L-2HB)/P(D-2HB)/PLLA/PDLA	F	50.0	-	-	208.3, 217.8	0.0	58.4	58.4	68.8

[d] Overall crystallinity estimated by WAXD.

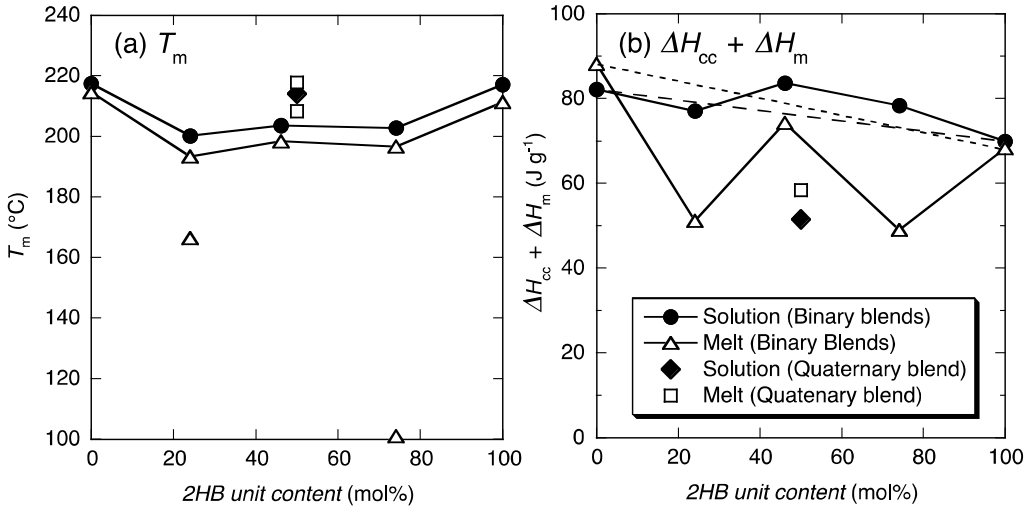

Figure 5. Melting temperature (T_m) (a) and enthalpy (ΔH_m) of blends as a function of 2HB unit content. The theoretical ΔH_m values are shown in Figure 5(b) with broken and dotted lines for the solution- and melt-crystallized blends, respectively.

The T_m values of P(L-2HB)/P(D-2HB) HMSC crystallites for the solution- and melt-crystallized

P(L-2HB)/P(D-2HB) blends at 2HB unit content of 100 mol% were 217.2 and 211.3 °C, respectively, whereas the T_m values of PLLA/PDLA HMSC crystallites for the solution- and melt-crystallized PLLA/PDLA blends at 2HB content of 0 mol% were 217.4 and 214.6 °C, respectively. The T_m values of stereocomplex crystallites composed of quaternary and ternary monomer units in the solution- and melt-crystallized P(L-2HB)/P(D-2HB-DLA), P(L-2HB-LLA)/P(D-2HB-DLA), and PLLA/P(D-2HB-DLA) blends (193.4–203.6°C) at 2HB content of 24.1–74.1mol% were lower than those of T_m values of P(L-2HB)/P(D-2HB) and PLLA/PDLA HMSC crystallites at 2HB content of 100 and 0 mol%. These decreases in T_m values for the blends containing the copolymer P(D-2HB-DLA) are attributable to the increased the lattice disorder in stereocomplex crystallites compared to those of the blends composed only of the homopolymers. On the other hand, the melt-crystallized quaternary polymer blend had two T_m values of 208.3 and 217.3°C, corresponding to those of P(L-2HB)/P(D-2HB) HMSC and PLLA/PDLA HMSC crystallites, respectively. In the case of the solution-crystallized quaternary polymer blend, although both P(L-2HB)/P(D-2HB) HMSC and PLLA/PDLA HMSC crystallites were present, the higher temperature melting peak of PLLA/PDLA HMSC crystallites overlapped with the lower temperature one of P(L-2HB)/P(D-2HB) HMSC crystallites and thereby could not be observed as a separate one.

The $\Delta H_c + \Delta H_m$ values of HMSC crystallites of the solution- and melt-crystallized P(L-2HB)/P(D-2HB) binary polymer blends at P(2HB) content of 100 mol% were 69.9 and 68.3 J g^{-1}, respectively, whereas those of the solution- and melt-crystallized PLLA/PDLA binary polymer blends at 2HB unit content of 0 mol% were 82.2 ad 88.2 J g^{-1}, respectively. The $\Delta H_c + \Delta H_m$ values of other solution-crystallized binary polymer blends containing at least one copolymer were 77.1, 83.7, and 78.4 J g^{-1} for 2HB unit contents of 24.1, 46.1, and 74.1 mol%, respectively, which were higher than or comparable with theoretical values. The theoretical values were calculated from the experimental $\Delta H_c + \Delta H_m$ values of PLLA/PDLA HMSC and P(L-2HB)/P(D-2HB) HMSC crystallites in the PLLA/PDLA and P(L-2HB)/P(D-2HB) binary polymer blends at 2HB unit contents of 0 and 100 mol%, respectively, assuming that two types of HMSC crystallites are formed without interaction between

them. The theoretical values are shown in Figure 5(b) with broken and dotted lines for the solution- and melt- crystallized blends, respectively. This finding confirms that the facile stereocomplexation of quaternary or ternary monomer units in the presence of solvent in the solution-crystallized binary polymer blends.

The $\Delta H_c + \Delta H_m$ values of other melt-crystallized binary polymer blends containing at least one copolymer were 49.0, 74.3, and 51.1 J g^{-1} for 2HB unit contents of 24.1, 46.1, and 74.1 mol%, which are respectively much lower than, comparable with, and much lower than theoretical values. The theoretical values were calculated from the experimental $\Delta H_c + \Delta H_m$ values of PLLA/PDLA and P(L-2HB)/P(D-2HB) HMSC crystallites in the melt-crystallized PLLA/PDLA and P(L-2HB)/P(D-2HB) binary polymer blends at 2HB unit content = 0 and 100 mol%. The rather disturbed crystallization at 2HB unit contents of 24.1 and 74.1 mol% can be ascribed to the phase separation between P(D-2HB-DLA) and PLLA or P(L-2HB) due to low miscibility between 2HB and LA unit sequences, which is evidence by the phase-separated structure of hetero-stereocomplexationable PLLA/P(D-2HB) or PDLA/P(L-2HB) blend[71,73] and weakened the interaction between the two polymer resulting in slower crystallization. Such slow crystallization is evidenced by low spherulite growth rage (G) stated in the following section. The relatively low $\Delta H_c + \Delta H_m$ values at 2HB unit contents of 24.1 and 74.1 mol% should be due to the same reason as stated above for the relatively low X_c values. In contrast, the rather high $\Delta H_c + \Delta H_m$ or X_c values of the solution-crystallized binary polymer blends at 2HB unit contents of 24.1 and 74.1 mol% should have been attained by the presence of solvent which disturbed the phase-separation between the homopolymer and the copolymer. For the solution- and melt-crystallized quaternary polymer blends, $\Delta H_c + \Delta H_m$ values were 51.5 and 58.4 J g^{-1}, respectively, which were much lower than the theoretical values. Considering the fact that the X_c values of the quaternary polymer blends were similar to the theoretical values, it is likely that the formation of both crystallites reduced the crystalline size of either or both HMSC crystallites, resulting in the seemingly low $\Delta H_c + \Delta H_m$ values of the quaternary polymer blends.

The DSC results here showed that the T_m values of the solution- and melt-crystallized binary polymer blends composed of at least one copolymer were lower than those of P(L-2HB)/P(D-2HB) and PLLA/PDLA HMSC crystallites in the solution- and melt-crystallized binary homopolymer blends of P(L-2HB)/P(D-2HB) and PLLA/PDLA, whereas the T_m values of P(L-2HB)/P(D-2HB) and PLLA/PDLA HMSC crystallites in the quaternary polymer blend were respectively lower than those in the P(L-2HB)/P(D-2HB) and PLLA/PDLA binary homopolymer blends, except for the T_m value of PLLA/PDLA HMSC crystallites in the melt-crystallized quaternary polymer blend. Also, the $\Delta H_c + \Delta H_m$ values showed the similar trend with the X_c values, except for the $\Delta H_c + \Delta H_m$ values of the solution- and melt-crystallized quaternary homopolymer blends, which were much lower than the theoretical values.

3.3 Polarized optical microscopy

To investigate the crystalline morphology and crystallization rate of the blends, polarized optical microscopic observation was performed. Figure 6 shows the polarized photomicrographs of the blends isothermally crystallization at 160°C for 6 min from the melt, except for 7 min of PLLA/P(D-2HB-DLA) blend (D). The binary polymer blends containing at least one homopolymer, i.e., P(L-2HB)/P(D-2HB) blend (A), P(L-2HB)/P(D-2HB-DLA) blend (B), P(L-2HB-LLA)/P(D-2HB-DLA) blend (C), PLLA/PDLA blend (E) are composed of the spherulites with well-defined Maltese crosses, whereas PLLA/P(D-2HB-DLA) binary blend (D) had the disordered spherultites without well-defined Maltese crosses and the quaternary polymer blend (F) consisted of the complicated spherulites with two types of morphologies depending on the direction and length from the spherulite center. The disordered spherultites of PLLA/P(D-2HB-DLA) blend (D) are attributable to the distorted stereocomplex crystalline lattice caused by the incorporation of rather large D-2-hydroxybutanoic acid units in the small L- and D-lactic acid units of PLLA/PDLA HMSC lattice. As elucidated by WAXD measurements, the quaternary polymer blends had two types of HMSC crystallites, which should be the cause for two types of morphologies. The spherulite

radius of binary and quaternary polymer blends are plotted in Figure 7(a) and (b), respectively, as a function of crystallization time (t_c). As the growth rate of the quaternary polymer blend depended on the direction from the spherulitic center, we selected two representative directions, right-hand and upper left-hand directions, which are shown with two red arrows in Figure 6(F). The radius of binary copolymer blends increased linearly with t_c, whereas that of the quaternary polymer blend depended on the direction for estimation; the radius increased linearly with t_c for upper left-hand direction but radius growth slowed down gradually with t_c for the right-hand direction.

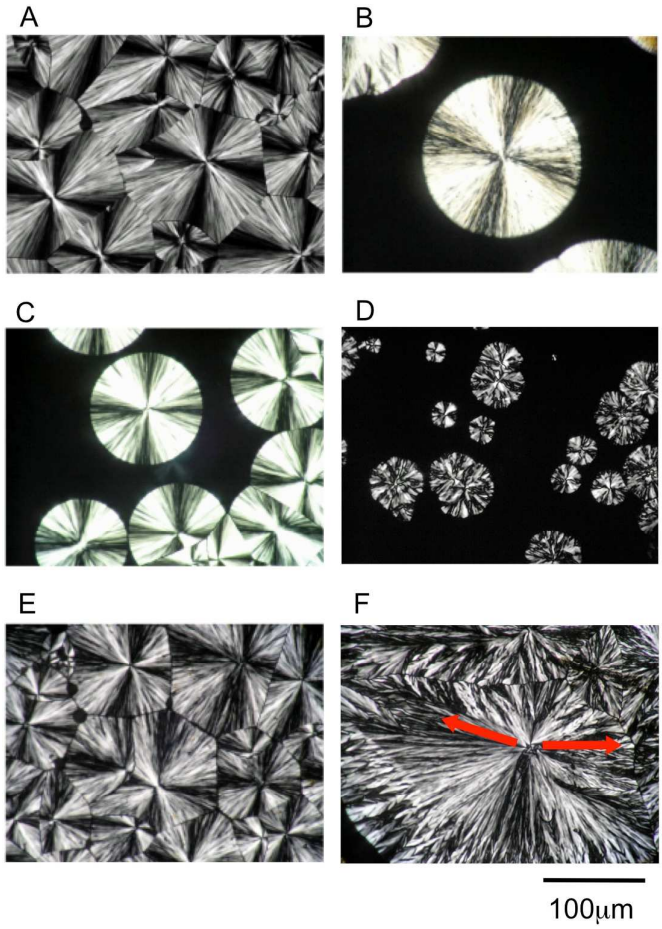

Figure 6. Polarized photomicrographs of binary polymer blends (A-E) and quaternary polymer blend (F) crystallized at T_c = 160°C for 6 min (A, B, C, E, F) and 7 min (D) from the melt. A: P(L-2HB)/P(D-2HB) blend, B: P(L-2HB)/P(D-2HB-DLA) blend, C: P(L-2HB-LLA)/P(D-2HB-DLA) blend, D: PLLA/P(D-2HB-DLA) blend, E: PLLA/PDLA blend, F: P(L-2HB)/P(D-2HB)/PLLA/PDLA blend. The radius growth was observed for two directions shown with two red arrows.

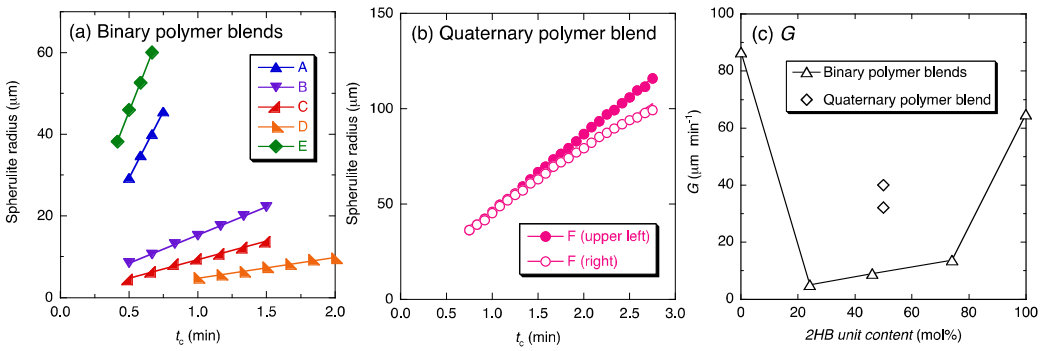

Figure 7. Spherulite radius of binary polymer blends (a) and quaternary polymer blend (b) as a function of crystallization time (t_c) and radial growth rate of spherulites (G) of blends as a function of 2HB unit content (c). A: P(L-2HB)/P(D-2HB) blend, B: P(L-2HB)/P(D-2HB-DLA) blend, C: P(L-2HB-LLA)/P(D-2HB-DLA) blend, D: PLLA/P(D-2HB-DLA) blend, E: PLLA/PDLA blend, F: P(L-2HB)/P(D-2HB)/PLLA/PDLA blend.

The radial growth rate of spherulites (G) of the blends crystallized at T_c = 160°C from the melt was obtained from Figure 7(a) and (b), assuming the linear increase of radius and thus obtained G values are plotted in Figures 7(c) as a function of 2HB unit content. The G values of the binary polymer blends composed of at least one copolymer, P(L-2HB)/P(D-2HB-DLA), P(L-2HB-LLA)/P(D-2HB-DLA), PLLA/P(D-2HB-DLA) blends at 2HB unit contents of 24.1, 46.1 and 74.1 mol%, were 5.1, 9.0, and 13.8 μm min^{-1}, respectively, were much lower than the those of the binary homopolymer blends of P(L-2HB)/P(D-2HB) and PLLA/PDLA were 64.9 and 86.7 μm min^{-1}. This can be expected from the fact that normally the crystallization rates of copolymers are lower than those calculated form the crystallization rate of homopolymers, assuming the linear dependence on comonomer unit content. Actually, the experimental G values of P(L-2HB-LLA) copolymers were much lower than those calculated from the experimental G values of P(L-2HB) and PLLA homopolymers.[79] On the other hand, both G values of the quaternary homopolymer blend (32.2 and 40.1 μm min^{-1}) were lower than the those of the binary homopolymer blends of P(L-2HB)/P(D-2HB) or PLLA/PDLA but higher than those of the binary polymer blends composed of at least one copolymer. The selection of P(L-2HB)/P(D-2HB) or PLLA/PDLA segments or chains at the growth

sites of P(L-2HB)/P(D-2HB) or PLLA/PDLA HMSC crystallites in the quaternary polymer blend should have reduced the *G* values compared to the P(L-2HB)/P(D-2HB) or PLLA/PDLA binary homopolymer blends, wherein there is no need for selecting the segments or chains although L- and D-polymer segments or chains should be alternately stacked on the growth sites. However, the selection effects in the quaternary polymer blend were not so large to reduce *G* values to below those of the binary polymer blends containing at least one copolymer, wherein cocrystallization of quaternary or ternary monomers occurs.

To confirm the presence of two crystalline species with different T_m values in the quaternary polymer blend, the sample crystallized at 160°C was directly heated at 10°C min^{-1} and its morphological change was observed (Figure 8). As a reference, the magnified DSC thermogram of melt-crystallized P(L-2HB)/P(D-2HB)/PLLA/PDLA quaternary polymer blend around T_m is shown in Figure 8, but it should be noted that there should be the slight gaps of transition temperatures between DSC and POM methods. No change was observed during heating up to 190°C, the melting of some domains of spherulites started and completed at 205 and 213°C, respectively, and all the spherulites melted at 226°C. Considering the higher T_m value of PLLA/PDLA HMSC crystallites in the melt-crystallized PLLA/PDLA binary polymer blend (214.6°C) than that of P(L-2HB)/P(D-2HB) HMSC crystallites in the melt-crystallized P(L-2HB)/P(D-2HB) binary polymer blend (211.3°C), the domains melted at high and low temperatures were composed of PLLA/PDLA and P(L-2HB)/P(D-2HB) HMSC crystallites, respectively. From the photo taken at 210°C, it is found that the two types of domains having P(L-2HB)/P(D-2HB) and PLLA/PDLA HMSC crystallites were irregularly located. It is likely that the phase separation into the domains of P(L-2HB) and P(D-2HB) and of PLLA and PDLA took place before spherulite formation although further phase-separation could have occurred during spherulite formation, and only PLLA/PDLA HMSC crystalline domains remained unmelted were observed at 210°C in Figure 9. The POM observation here indicated the *G* values of the binary polymer blends composed of at least one copolymer and of the quaternary polymer blend were lower than those of P(L-2HB)/P(D-2HB) and PLLA/PDLA binary homopolymer blends.

The quaternary polymer blend was phase-separated into two types of domains consisted of P(L-2HB) and P(D-2HB) and of PLLA and PDLA and then there the spherulites composed of P(L-2HB)/P(D-2HB) and PLLA/PDLA HMSC crystallites were formed.

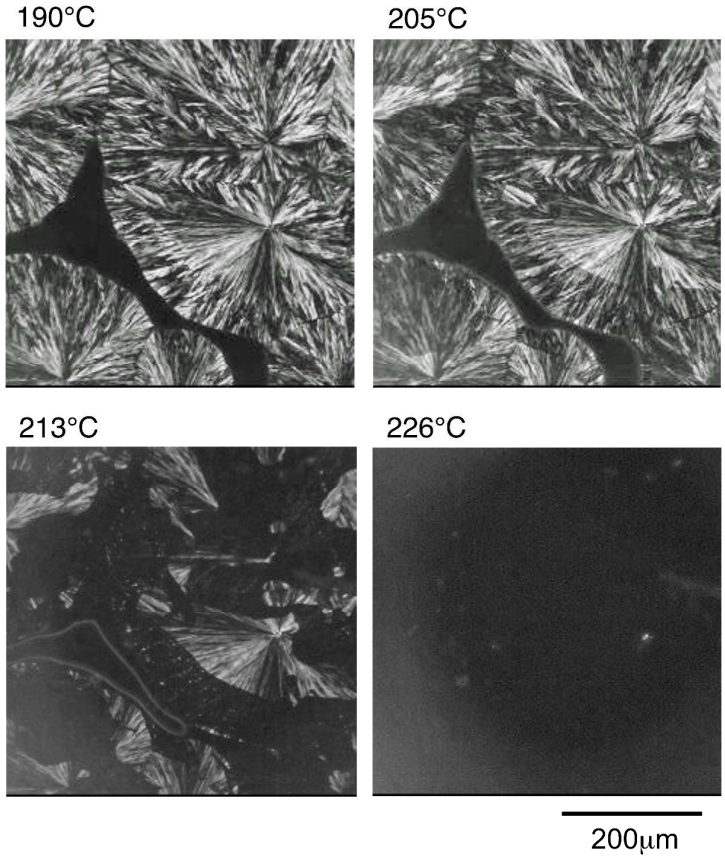

Figure 8. Polarized photomicrographs of P(L-2HB)/P(D-2HB)/PLLA/PDLA quaternary polymer blends obtained at the indicated temperatures during heating from 160°C, together with magnified DSC thermogram of P(L-2HB)/P(D-2HB)/PLLA/PDLA quaternary polymer blends around T_m.

4 Conclusions

The WAXD profiles and the *d* values estimated from WAXD measurements first revealed the stereocomplexation of quaternary or ternary monomer units in enantiomeric binary polymer blends containing the copolymer composed of optically active 2HB and LA units [P(L-2HB)/P(D-2HB-DLA), P(L-2HB-LLA)/P(D-2HB-DLA), and PLL/P(D-2HB-DLA) blends] and the dual stereocomplxation in P(L-2HB)/P(D-2HB)/PLLA/PDLA quaternary homopolymer blend. The X_c and $\Delta H_c + \Delta H_m$ values of solution-crystallized binary polymer blends composed of at least one copolymer were higher than or comparable with those calculated values, whereas the X_c and $\Delta H_c + \Delta H_m$ values of melt-crystallized binary polymer blends composed of the homopolymer and the copolymer [P(L-2HB)/P(D-2HB-DLA) and PLL/P(D-2HB-DLA) blends] were lower than the calculate values and the X_c and $\Delta H_c + \Delta H_m$ values of the melt-crystallized binary polymer blends composed of the two copolymers [P(L-2HB-LLA)/P(D-2HB-DLA) blend] were comparable with the theoretical values. The X_c values of the solution- and melt-crystallized quaternary homopolymer blends were respectively slightly lower and higher than those of the theoretical values, whereas the $\Delta H_c + \Delta H_m$ values of the solution- and melt-crystallized quaternary homopolymer blends were much lower than the theoretical values, probably due to the decreased crystalline size of either or both HMSC crystallites. The T_m values of the solution- and melt-crystallized binary polymer blends composed of at least one copolymer were lower than those of P(L-2HB)/P(D-2HB) and PLLA/PDLA HMSC crystallites in the solution- and melt-crystallized binary homopolymer blends of P(L-2HB)/P(D-2HB) and PLLA/PDLA, whereas the T_m values of P(L-2HB)/P(D-2HB) and PLLA/PDLA HMSC crystallites in the quaternary polymer blend were respectively lower than those in the P(L-2HB)/P(D-2HB) and PLLA/PDLA binary homopolymer blends, except for the T_m value of PLLA/PDLA HMSC crystallites in the

melt-crystallized quaternary polymer blend. The *G* values of the binary polymer blends composed of at least one copolymer and of the quaternary polymer blend were lower than those of P(L-2HB)/P(D-2HB) and PLLA/PDLA binary homopolymer blends. The quaternary polymer blend was phase-separated into two types of domains consisted of P(L-2HB) and P(D-2HB) and of PLLA and PDLA and then there the spherulites composed of P(L-2HB)/P(D-2HB) and PLLA/PDLA HMSC crystallites were formed.

Acknowledgements: This research was supported by JSPS KAKENHI Grant Number 24550251 and MEXT KAKENHI Grant Number 24108005.

References

1. M. Vert, J. Feijen, A. -C. Albertsson, G. Scott and E. Chiellini, editors, Biodegradable polymers and plastics, Cambridge: Royal Society of Chemistry, 1992.
2. D. P. Mobley, editor, Plastics from microbes, New York: Hanser Publishers, 1994.
3. M. Vert, G. Schwarch and J. Coudane, *J. Macromol. Sci. Pure Appl. Chem.*, 1995, **A32**, 787–96.
4. A. J. Domb, J. Kos and D. M. Wieseman, editors, Handbook of biodegradable polymers (Drug Targeting and Delivery, vol. 7), Amsterdam (The Netherlands): Harwood Academic Publishers, 1997.
5. D. L. Kaplan, editor, Biopolymers from renewable resources, Springer: Berlin (Germany), 1998.
6. D. Garlotta, *J. Polym. Environ*., 2001, **9**, 63–84.
7. A. Södergård and M. Stolt , *Prog. Polym. Sci.*, 2002, **27**, 1123–63.
8. A. -C. Albertsson, editor, Degradable aliphatic polyesters (Advances in Polymer Science, Vol.157); Berlin (Germany): Springer, 2002.
9. Y. Doi and A. Steinbüchel, editors, Polyesters I, II, III (Biopolymers, Vol. 3a, 3b, 4), Weinheim (Germany): Wiley-VCH, 2002.
10. R. Auras, L. -T. Lim, S. E. M. Selke and H. Tsuji, editors., Poly(lactic acid): Synthesis, structures, properties, processing, and applications (Wiley Series on Polymer Engineering and Technology), New Jersey: John Wiley & Sons, Inc., 2010.
11. D. Grenier, R. E. Prud'homme, *J. Polym. Sci. Polym. Phys. Ed.*, 1984, **22**, 577–587.
12. R. Voyer, R. E. Prud'homme, *Eur. Polym. J.* 1989, **25**, 365–369.
13. Y. Ikada, K. Jamshidi, H. Tsuji and S. H. Hyon, *Macromolecules*, 1987, **20**, 904–906.
14. J. Slager and A. J. Domb. *Adv. Drug. Delivery. Rev.*, 2003, **55**, 549–583.
15. H. Tsuji, *Macromol. Biosci.*, 2005, **5**, 569–597.
16. K. Fukushima and Y. Kimura, *Polym. Int.* 2006, **55**, 626–642.
17. M. Kakuta, M. Hirata and Y. Kimura, *Polym Rev.* 2009, **49**, 107–140.
18. P. Pan and Y. Inoue, *Prog. Polym. Sci.*, 2009, **34**, 605–640.
19. H. Tsuji and Y. Ikada, In: Yu L, editor, Biodegradable polymer blends from renewable resources, New Jersey: John Wiley & Sons, Inc., 2009; p. 165–190.
20. S. Saeidlou, M. A. Huneault, H. Li and C. B. Park, *Prog. Polym. Sci.*, 2012, **37**, 1657–1677.
21. H. Tsuji and A.Okumura, *Macromolecules*, 2009, **42**, 7263–7266.
22. H. Tsuji and A. Okumura, *Polym. J.*, 2011, **43**, 317–324.
23. Tsuji H and S. Shimizu, *Polymer*, 2012, **53**, 5385–5392.
24. Andersson SR, Hakkarainen M, Albertsson A-C. Polymer 2013; 54: 4105–4111.
25. H. Tsuji and Y. Ikada, *Polymer*, 1999, **40**, 6699–6708.

26. H. Tsuji, *Polymer*, 2000, **41**, 3621–3630.
27. H. Tsuji and I. Fukui, *Polymer*, 2003, **44**, 2891–2896.
28. H. Tsuji and T. Tsuruno, *Macromol. Mater. Eng.*, 2010, **295**, 709–715.
29. H. Tsuji, Y. Ikada, S. H. Hyon, Y. Kimura and T. Kitao, *J. Appl. Polym. Sci.*, 1994, **51**, 337–344.
30. M. Takasaki, H. Ito and T. Kikutani, *J. Macromol. Sci. Phys.*, 2003, **42 B (3-4 SPEC.)**, 403–420.
31. N. Kang, M. -È. Perron, R. E. Prud'homme, Y. Zhang, G. Gaucher and J. -C. Leroux, *Nano Lett.,* 2005, **5**, 315–319.
32. J. Zhang, K. Tashiro, H. Tsuji and A. J. Domb, *Macromolecules,* 2007, **40**, 1049–1054.
33. M. Fujita, T. Sawayanagi, H. Abe, T. Tanaka, T. Iwata, K. Ito, T. Fujisawa and M. Maeda, *Macromolecules*, **2008**, *41*, 2852–2858.
34. H. Tsuji, M. Nakano, M. Hashimoto, K. Takashima, S. Katsura and A. Mizuno, *Biomacromolecules*, 2006, **7**, 3316–3320.
35. D. Ishii, T. H. Ying, T. H. A. Mahara, S. Murakami, T. Yamaoka, W. Lee and T. Iwata, *Biomacromolecules*, 2009, **10**, 237–242.
36. M. Spasova, N. Manolova, D. Paneva, R. Mincheva, P. Dubois, I. Rashkov and V. Maximova, D. Danchev, *Biomacromolecules*, 2010, **11**, 151–159.
37. Y. Furuhashi and N. Yoshie, *Polym. Int.*, 2012, **6**, 301–306.
38. P. Purnama and S. H. Kim, *Macromolecules*, 2010, **43**, 1137–1142.
39. H. Tsuji and S. Yamammoto, *Macromol. Mater. Eng.,* 2011, **296**, 583–589.
40. H. Tsuji and L. Bouapao, *Polym. Int.*, 2012, **61**, 442–450.
41. T. Akagi, T. Fujiwara and M. Akashi, *Angew. Chem. Int. Ed.*, 2012, **51**, 5493–5496.
42. P. Purnama and S. Hyun Kim, *Polym. Int.*, 2012, **61**, 939–942.
43. S. R. Andersson, M. Hakkarainen, S. Inkinen, A. Södergård, and A. -C. Albertsson, *Biomacromolecules*, 2012, **13**, 1212–1222.
44. B. Na, J. Zhu, R. Lv, Y. Ju, R. Tian and B. Chen, *Macromolecules*, 2014, **47**, 347–352.
45. X. Wang and R. E. Prud'homme, *Macromolecules*, 2014, **47**, 668–676.
46. Y. Li, C. Han, X. Zhang, Q. Dong and L. Dong, *Thermochim. Acta*, 2013, **573**, 193–199.
47. H. Ajiro, Y. -J. Hsiao, H. T. Tran, T. Fujiwara and M. Akashi, *Macromolecules*, 2013, **46**, 5150–5156.
48. H. Marubayashi, T. Nobuoka, S. Iwamoto, A. Takemura and T. Iwata, *ACS Macro. Lett.*, 2013, **2**, 355–360.
49. N. Yui, P. J. Dijkstra and J. Feijen. J. *Makromol. Chem.*, 1990, **191**, 481–488.
50. N. Spassky, M. Wisniewski, C. Pluta and A. Le Borgne, *Makromol. Chem. Phys.,* 1996, **197**, 2627–2637.

51. M. Spinu, C. Jackson, M. Y. Keating and K. H. Gardner, *J. Macromol. Sci. Part A: Pure Appl. Chem.*, 1996, **33**, 1497–1530.
52. J. -R. Sarasua, R. E. Prud'homme, M. Wisniewski, A. Le Borgne and N. Spassky, *Macromolecules*, 1998, **31**, 3895–3905.
53. T. M. Ovitt and G. W. Coates, *J. Am. Chem. Soc.*, 2002, **124**, 1316–1326.
54. L. Li, Z. Zhong, W. H. De Jeu, P. J. Dijkstra and J. Feijen, *Macromolecules,* 2004, **37**, 8641–8646.
55. J. Hu, Z. Tang, X. Qiu, X. Pang, Y. Yang, X. Chen and X. Jing, *Biomacromolecules,* 2005, **6**, 2843–2850.
56. Z. Tang, Y. Yang, X. Pang, J. Hu, X. Chen, N. Hu and X. Jing, *J. Appl. Polym. Sci.*, 2005, **98**, 102–108.
57. K. Fukushima, Y. Furuhashi, K. Sogo, S. Miura and Y. Kimura Y. *Macromol. Biosci.*, 2005, **5**, 21–29.
58. K. Fukushima, M. Hirata and Y. Kimura, *Macromolecules*, 2007, **40**, 3049–3055.
59. K. Fukushima and Y. Kimura, *J. Polym. Sci. Part A: Polym. Chem.*, 2008, **46**, 3714–3722.
60. S. H. Kim, F. Nederberg, L. Zhang, C. G. Wade, R. M. Waymouth, J. L. Hedrick, *Nano Lett.,* 2008, **8**, 294–301.
61. F . Nederberg, E. Appel, J. P. K. Tan, H. K. Sung, K. Fukushima, J. Sly, R. D. Miller, R. M. Waymouth, Y. Y. Yang and J. L. Hedrick, *Biomacromolecules*, 2009, **10**, 1460–1468.
62. M. Hirata, K. Kobayashi and Y. Kimura, *J. Polym. Sci. Part A: Polym. Chem.*, 2010, **48**, 794–801.
63. H. Tsuji, T. Wada, Y. Sakamoto and Y. Sugiura, *Polymer*, 2010, **51**, 4937–4947.
64. K. Masutani, C.W. Lee and Y. Kimura, *Macromol. Chem. Phys*., 2012, **213**, 695–704.
65. K. Masutani, C.W. Lee and Y. Kimura, *Polymer*, 2012, **53**, 6053–6062.
66. M. H. Rahaman and H. Tsuji, *Macromol. React. Eng.,* 2012, **6**, 446–457.
67. T. Isono, Y. Kondo, I. Otsuka, Y. Nishiyama, R. Borsali, T. Kakuchi, T. Satoh, *Macromolecules*, 2013, **46**, 8509–8518.
68. M. H. Rahaman and H. Tsuji, *J. Appl. Polym. Sci.*, 2013, **129**, 2502–2517.
69. K. Masutani, C. W. Lee and Y. Kimura, *Polym. J.*, 2013, **45**, 427–435.
70. M. H. Rahaman and H. Tsuji, *Polym. Degrad. Stab.*, 2013, **98**, 709–719.
71. H. Tsuji, S. Yamamoto, A. Okumura and Y. Sugiura, *Biomacromolecules*, 2010, **11**, 252–258.
72. H. Tsuji, K. Shimizu, Y. Sakamoto and A. Okumura, *Polymer*, 2011, **52**, 1318–25.
73. H. Tsuji, F. Deguchi, Y. Sakamoto and S. Shimizu, *Macromol. Chem. Phys.,* 2012, **213**, 2573–2581.

74. H. Tsuji and M. Suzuki, *Macromol. Chem. Phys.*, 2014, **215**, 1879–1888.
75. H. Tsuji and T. Hayakawa, *Polymer*, 2014, **55**, 721–726.
76. H. Tsuji, M. Hosokawa and Y. Sakamoto, *ACS Macro. Lett.*, 2012, **1**, 687–91.
77. H. Tsuji, M. Hosokawa and Y. Sakamoto, *Polymer*, 2013, **54**, 2190–2198.
78. H. Tsuji and T. Tawara, *Polymer*, 2015, **68**, 57–64.
79. H. Tsuji and T. Sobue, *Polymer*, 2015, **72**, 202–211.
80. H. Tsuji and H. Matsuoka, *Macromol. Rapid Commun.*, 2008, **2**, 1372–1377.
81. H. Tsuji, H. Matsuoka and S. Itsuno, *J. Appl. Polym. Sci.*, 2008, **110**, 3954–3962.
82. P. Pan, B. Zhu, W. Kai, T. Dong, Y. Inoue, *J. Appl. Polym. Sci.*, 2008, **107**, 54–62.
83. P. Pan, W. Kai, B. Zhu, T. Dong, Y. Inoue, *Macromolecules*, 2007, **40**, 6898–905.

Figure captions

Figure 1. Molecular structures of poly(L-2-hydroxybutanoic acid) [P(L-2HB)], poly(D-2-hydroxybutanoic acid) [P(D-2HB)], poly(L-2-hydroxybutanoic acid-L-lactic acid) [P(L-2HB-LLA)], and poly(D-2-hydroxybutanoic acid- D-lactic acid) [P(D-2HB-DLA)], poly(L-lactic acid) (PLLA), and poly(D-lactic acid) (PDLA), and their combinations for blends. (A), (B), (C), (D), and (E) correspond to the blend codes in the present study.

Figure 2. WAXD profiles of solution-crystallized (a) and melt-crystallized (T_c = 160°C) (b) binary polymer blends (A–E) and quaternary polymer blend (F). A: P(L-2HB)/P(D-2HB) blend, B: P(L-2HB)/P(D-2HB-DLA) blend, C: P(L-2HB-LLA)/P(D-2HB-DLA) blend, D: PLLA/P(D-2HB-DLA) blend, E: PLLA/PDLA blend, F: P(L-2HB)/P(D-2HB)/PLLA/PDLA blend. Dotted and broken lines indicate the crystalline diffraction angles for P(L-2HB)/P(D-2HB) and PLLA/PDLA HMSC crystallties, respectively.

Figure 3. Interplane distance (d) (a) and crystallinity (X_c) (b) of solution- and melt-crystallized (T_c = 160°C) blends in the ranges of 7.4–8.3 and 3.7–4.2Å as a function of 2HB unit content. The theoretical d values are shown in Figure 3(a) with broken lines, whereas the theoretical X_c values are shown in Figure 3(b) with broken and dotted lines for the solution- and melt-crystallized blends, respectively.

Figure 4. DSC thermograms of solution-crystallized (a) and melt-crystallized (T_c = 160°C) (b) binary polymer blends (A–E) and quaternary polymer blend (F). A: P(L-2HB)/P(D-2HB) blend, B: P(L-2HB)/P(D-2HB-DLA) blend, C: P(L-2HB-LLA)/P(D-2HB-DLA) blend, D: PLLA/P(D-2HB-DLA) blend, E: PLLA/PDLA blend, F: P(L-2HB)/P(D-2HB)/PLLA/PDLA blend.

Figure 5. Melting temperature (T_m) (a) and enthalpy (ΔH_m) of blends as a function of 2HB unit content. The theoretical ΔH_m values are shown in Figure 5(b) with broken and dotted lines for the solution- and melt-crystallized blends, respectively.

Figure 6. Polarized photomicrographs of binary polymer blends (A-E) and quaternary polymer blend (F) crystallized at T_c = 160°C for 6 min except for D (7 min) from the melt. A: P(L-2HB)/P(D-2HB) blend, B: P(L-2HB)/P(D-2HB-DLA) blend, C: P(L-2HB-LLA)/P(D-2HB-DLA) blend, D:

PLLA/P(D-2HB-DLA) blend, E: PLLA/PDLA blend, F: P(L-2HB)/P(D-2HB)/PLLA/PDLA blend. The radius growth was observed for two directions shown with two red arrows.

Figure 7. Spherulite radius of binary polymer blends (a) and quaternary polymer blend (b) as a function of crystallization time (t_c) and radial growth rate of spherulites (G) of blends as a function of 2HB unit content (c).

Figure 8. Polarized photomicrographs of P(L-2HB)/P(D-2HB)/PLLA/PDLA quaternary polymer blends obtained at the indicated temperatures during heating from 160°C, together with magnified DSC thermogram of P(L-2HB)/P(D-2HB)/PLLA/PDLA quaternary polymer blends around T_m.